Zero Torque Pulsation of Surface Permanent Magnet Synchronous Motor for Ship Gyro Stabilizer by Pole/Slot Number and Air-gap Designs

Sun-Kwon Lee[1,2], Gyu-Hong Kang[1], *Senior Member IEEE* and Jin Hur[2], *Senior Member IEEE* and Byoung-Woo Kim[2]
[1]Korea Marine Equipment Research Institute, SongJeong-Dong, GangSeo-Gu, Busan, 1631-10, Korea
[2]Dept. of Electrical Engineering, University of Ulsan, 102. Street Dae-hak, Nam-gu, Ulsan 680-749, Korea
sunkwonlee@komeri.re.kr

***Abstract*—This paper deals with the reduction of torque pulsation including torque ripple and cogging torque in surface permanent magnet (SPM) brushless AC motors. The fractional combination and air-gap shape design by shaping the permanent magnet (PM) and stator core are studied to reduce torque pulsation. The torque ripple reduction is achieved by adjusting magnetic flux density in air-gap contour. The zero torque pulsation means the ripple ratio to average torque below 0.5%. The magnetic field and torque characteristics are analyzed by 2 dimensional (2D) finite element analysis (FEA) and prototype to validate is manufactured and measured.**

***Index Terms*—SPMSM, permanent magnet, torque pulsation, finite element analysis.**

I. Introduction

Marine applications have strict limits on vibrations and interference for electromagnetic comparability, and so high efficiency and low vibrations are key requirements [1]. PM machines with a fractional number of slots per pole and a concentrated winding have shorter end windings and lower overall length and yet have high efficiency, torque, and power density [1]-[3]. Further, the fractional slot machines have extremely low cogging torque without the need for design features such as skew [2].

Torque ripple caused by rotor field and stator current, is affected by harmonic components of radial flux density. The cogging torque is generated from the interaction between the air-gap flux density distribution and stator slotting. The torque pulsation reduction can be achieved by minimizing torque ripple and cogging torque [3].

Thus many previous studies [1]-[7] dealt with torque pulsation reduction approaches of PM machines. Hur and colleagues [4] proposed 3rd harmonic elimination method to reduce cogging torque. The analytical approach was introduced to calculate cogging torque of interior permanent magnet (IPM) motor [5]. Some researchers [6]-[7] studied IPM machines and some papers [6], [7] include optimization problems.

In this paper, the torque pulsation reduction is introduced by poles/slots combination and air-gap structure design using magnet shapes and stator core structure. The torque ripple reduction principle by adjusting magnetic flux density is also discussed. The torque pulsation is achieved almost zero against to average generated torque. 2D FEA is used to calculate the magnetic field of designed motor.

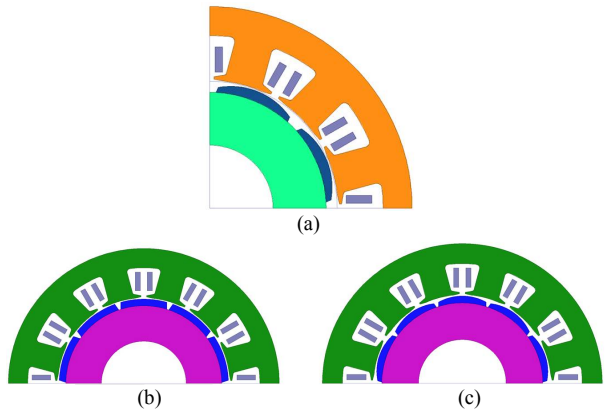

Fig. 1. Designed and analysis models. (a) 8 pole-12 slot model, (b) 10 pole-12 slot model1, (c) 10 pole-12 slot model2.

TABLE I
SPECIFICATIONS OF ANALYZED MODELS

Items	8p12s	10p12s	Unit
Poles-slots	8-12	10-12	-
Rotational speed	4000	4000	Rpm
Armature current	10	10	A
Stator Out Diameter	180	180	Mm
Stack Length	63	49/54	Mm
Residual Induction	1.21	1.21	T
Magnet type	Nd-Fe-B	Nd-Fe-B	-

II. Analysis Model Descriptions

Fig. 1 shows the cross sections of analyzed models. The identical stator with 12 slots concentrated windings is employed for each model. The detailed descriptions of analyzed models are listed in Table I. The differences between 10p12s model1 and model2 are permanent magnet shape and stack length. The stack length of model1 is modified to consider same current density. The 8p12s means the 8 pole-12 slot machine and 10p12s stands for 10 pole-12 slot machine.

III. Reduction of Torque Pulsation

Fig. 2 illustrates the cogging torque comparison among three models. In spite of straight magnet shape of 10p12s model1, the cogging torque reduces against to 8p12s machine. The rates of peak to peak value of cogging torque to average torque are 4.4% for 8p12s, 0.83% for 10p12s model1 and 0.14% for 10p12s model2, respectively.

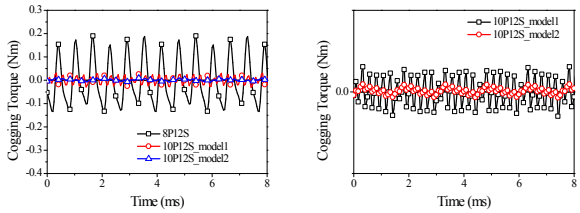

Fig. 2. Cogging torque analysis results.

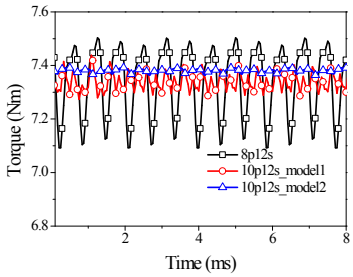

Fig. 3. Rated torque analysis results (Armature current : 10A).

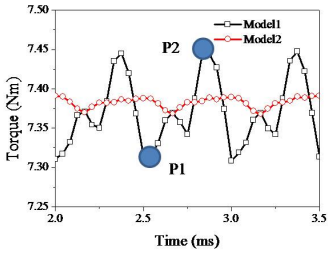

Fig. 4. Rotating torque behavior according to position.

Fig. 3 shows the torque ripple comparison results among three different models. The ratio of torque ripple to average torque of 8p12s model is 4.5% whereas 10p12s model1 is 1.8%. The final 10p12s models with partly enlarged air-gap by magnet cutting has lowest torque ripple among three models which is 0.31%.

The torque ripple can be reduced by upgrading torque value at minimum points and downsizing at maximum torque points [3] respectively as in Fig. 4. P1 (2.5ms) and P2 (2.83ms) mean the minimum and maximum torque point respectively. To solve the problem, the flux passing through the rotor pole should be reduced at minimum torque position. The air-gap torque distribution can be calculated by Maxwell stress tensor as (1).

$$P_t = \frac{B_n B_t}{\mu_0} \tag{1}$$

where, P_t : tangential components of force density; B_n : normal components of magnetic flux density on contour; B_t : tangential components of magnetic flux density on contour; μ_0 : magnetic permeability of air.

Fig. 5 shows the flux density distributions and air-gap flux density waveforms for each model at maximum and minimum torque generating position. Fig. 6 presents the tangential force density on air-gap contour of which summation is generated torque. Fig. 8 shows the prototype for 10p12s model2 and measured back electromotive force (EMF). The more useful data will be introduced in extended paper.

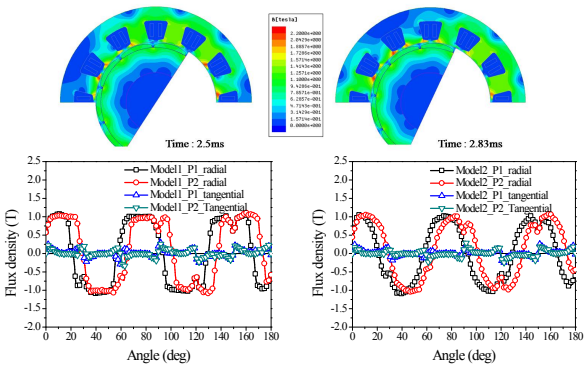

Fig. 5. Flux density distributions of each position (P1 : 2.5ms, P2 : 2.83ms).

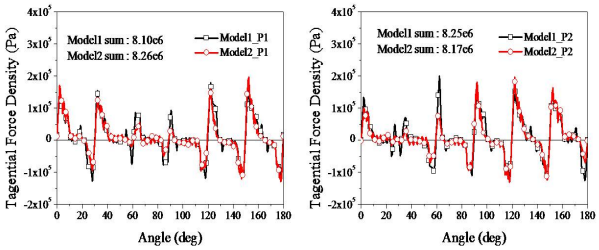

Fig. 6. Air-gap torque distribution analysis (P1 : 2.5ms, P2 : 2.83ms).

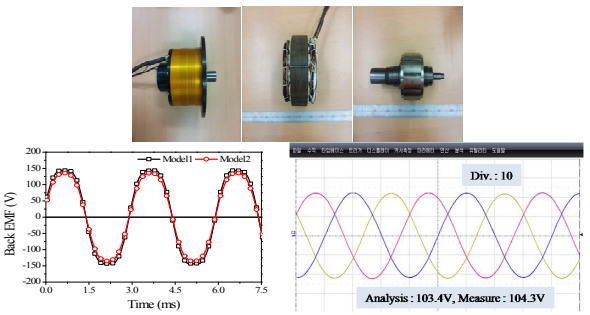

Fig. 7. Prototype of 10p12s model2 and back EMF comparison.

REFERENCES

[1] S. -K. Lee, G. -H. Kang, and J. Hur, "Finite element computation of magnetic vibration sources in 100kW two fractional-slot interior permanent magnet machines for ship", *IEEE Trans. Magn.*, vol. 48, no. 2, pp867-870, 2012.

[2] Z. Q. Zhu, D. Ishak, D. Howe, and J, Chen, "Unbalanced magnetic forces in permanent-magnet brushless machines with diametrically asymmetric phase windings", *IEEE Trans. Ind. Appl.*, vol. 43, no. 6, pp1544-1553, 2007.

[3] S. K. Lee, G. H. Kang, J. Hur, and B. W. Kim, "Stator and rotor shape designs of interior permanent magnet type brushless DC motor for reducing torque fluctuation", *IEEE Trans. Magn.*, vol. 48, no. 11, pp4662-4665, 2012.

[4] J. Hur, J.-W Reu, B.-W. Kim, and G.-H. Kang, "Vibration reduction of IPM-type BLDC motor using negative third harmonic elimination method of air-gap flux density", *IEEE Trans. Industry Applications,* vol. 47, no. 3, pp. 1300-1309, 2011.

[5] G.-H. Kang, J.-P. Hong, and G.-T. Kim, "Analysis of cogging torque in interior permanent magnet motor by analytical method", *KIEE Int. Trans. Electr. Mach. Energy Conver. Syst.,* vol. 11B, no. 2, pp. 1-8, 2006.

[6] L. Fang, S.-I. Kim, S.-O. Kwon, and J.-P. Hong, "Novel double-barrier rotor designs in interior-PM motor for reducing torque pulsation", *IEEE Trans. Magn.,* vol. 46, no. 6, pp. 2183-2186, 2010.

[7] N. Bianchi, S. Bolognani, D. Bon, and M. D. Pre, "Rotor flux-barrier design for torque ripple reduction in synchronous reluctance and PM-assisted synchronous reluctance motors", *IEEE Trans. Ind. Appl.,* vol. 45, no. 3, pp. 921-928, 2009.